



Protective effect of combined moxibustion and decoction therapy on Bleomycin-induced pulmonary fibrosis in rats under Nuclear Factor- κ B/Transforming Growth Factor- β 1/Smads signaling pathway

Shanjun Yang¹, Xiao Feng¹, Yue Wang¹, Yang Qu^{2*}, Luming Xing¹, Hao Wang¹, Yujia Zhang¹, Xiyao Li³

¹Department of Lung Disease, Second Affiliated Hospital of Heilongjiang University of Chinese Medicine, Harbin 150001, China

²Department of Internal Medicine Clinic (a), Second Affiliated Hospital of Heilongjiang University of Chinese Medicine, Harbin 150001, China

³First Clinical Medical College, Beijing University of Chinese Medicine, Beijing 100007, China ¹Department of Lung Disease, Second Affiliated Hospital of Heilongjiang University of Chinese Medicine, Harbin 150001, China

ARTICLE INFO

Original paper

Article history:

Received: January 12, 2022

Accepted: April 01, 2022

Published: June 30, 2022

Keywords:

Nuclear factor kappa B/transforming growth factor- β 1/Smads signaling pathway; bleomycin; pulmonary fibrosis; moxibustion; Bu Fei Qu Yu decoction.

ABSTRACT

It was aimed to discuss the effect of moxibustion (Mox) combined with Bu Fei Qu Yu (BFQY) decoction under the nuclear factor- κ B (NF- κ B)/transforming growth factor- β 1 (TGF- β 1)/Smads signaling pathway in the treatment of pulmonary fibrosis (PF). The PF rat models were prepared with bleomycin (BLM). They were divided into the normal (Nor) group, the PF model group (BLM puncture perfusion), the Mox group (grain-sized Mox at the back-shu points and Xuxiao points), the BFQY group (intra-gastrical BFQY decoction), and the Mox combined with BFQY decoction (Mox+BFQY) group. Lung tissue sections were prepared, and the hematoxylin-eosin (HE) staining and Masson staining were performed to observe the inflammatory response and the degree of PF. The contents of hydroxyproline (HYP), glutathione (GSH), and malondialdehyde (MDA), and the expressions of NF- κ B p65, TGF- β 1, Smad2, and Smad7 in lung tissues were detected. Compared with those in the Nor group, the inflammatory response score, PF degree score, HYP, GSH, and MDA contents, NF- κ B p65, TGF- β 1, and Smad2 expressions were significantly increased in the PF group, but Smad7 expression decreased ($P < 0.05$). The above symptoms were significantly improved in the Mox, BFQY, and Mox+BFQY groups ($P < 0.05$). The effect was more remarkable in the Mox+BFQY group, and there was no significant difference in each index compared with those in the Nor group ($P > 0.05$). Thus, the combined therapy of Mox and decoction had an effect on PF through the NF- κ B/TGF- β 1/Smads pathway.

Doi: <http://dx.doi.org/10.14715/cmb/2022.68.6.8>

Copyright: © 2022 by the C.M.B. Association. All rights reserved.

Introduction

Pulmonary fibrosis (PF) is the terminal manifestation of various interstitial lung diseases. The main pathological features are the destruction of the lung parenchyma and the accumulation of extracellular matrix in the interstitial and alveolar spaces of the lung (1). The clinical features of PF are mainly severe impairment of lung function, which can lead to respiratory failure and even death in severe cases. In recent years, the incidence of PF has shown an increasing trend, and the 5-year survival rate is as low as 50% (2). The etiology of PF is still unclear, the pathogenesis is very complex, and there is no clear and effective treatment method currently. Some researchers have reported that the lung tissue would repair itself when it is damaged. If the repairing function is abnormal, it will cause the abnormal expression of some cytokines, such as tumor necrosis factor- α (3). The biological processes like hypoxia, angiogenesis, and apoptosis also play important roles in the pathogenesis of PF (4).

Transforming growth factor- β 1 (TGF- β 1) is a class of cytokines recognized as an important factor leading to fibrosis, which mainly depends on the signaling pathway

mediated by the Smads and participates in the process of PF directly or indirectly (5). Nuclear factor- κ B (NF- κ B) is distributed in the cytoplasm, and the activated NF- κ B will enter the nucleus and induce the expression of related genes (6). It has been confirmed that NF- κ B is involved in the occurrence of lung diseases such as bronchial asthma, acute lung injury, and acute respiratory distress syndrome (7), but its mechanism of action in PF is still undefined.

At present, the drugs used for the prevention and treatment of PF mainly include TGF- β inhibitors, but there are some limitations, such as large rejection reactions after the treatment with different drugs (8). Therefore, seeking effective drugs for the prevention and treatment of PF has become a hot issue globally. Traditional Chinese medicine believes that the pathogenesis of PF is related to deficiency of healthy qi, turbid and heat toxins in the environment, etc. The main causes include external pathogens attacking the collateral channels, phlegm, blood stasis, and internal injuries blocking the collateral channels, and chronic illnesses infiltrating the collaterals, ultimately leading to collateral paralysis and collateral stasis (9). Moxibustion (Mox) can be adopted to treat refractory and chronic organ asthenic diseases by dredging the meridians and collate-

* Corresponding author. Email: xintou6079853@163.com

als, strengthening yang, and tonifying qi (10). Bu Fei Qu Yu (BFQY) decoction has the effects of invigorating the lungs and qi, promoting blood circulation, and removing blood stasis.

On this ground, the rat models with PF were prepared using bleomycin (BLM). They were treated with Mox, BFQY decoction, and a combination of Mox and the decoction, respectively. The effects of different treatment methods on PF in rats were observed, which included those on the inflammatory response, the degree of PF, and the NF- κ B/TGF- β 1/Smads signaling pathway. It was intended to provide an experimental basis for finding effective treatments for PF.

Materials and Methods

Grouping of experimental animals

Clean male Sprague-Dawley (SD) rats were selected as the research objects, and all the rats were purchased from Kaixue Biotechnology (Shanghai) Co., Ltd. 90 male rats were randomly divided into the normal (Nor) group, the PF model group, the Mox group, the BFQY decoction group, and the Mox+BFQY group. There were 10 rats in the normal group and 20 rats in each of the other groups. The general conditions of the rats were observed, and the body weight of the rats was weighed before and after modeling and treatment.

Treatment methods and processing

Except for the rats in the normal group, the rats in other groups were given 3mL/kg 3.5% chloral hydrate solution for anesthesia. The supine position was taken and the neck was sterilized. The skin was incised and other tissues were bluntly separated. After the trachea of the rat was fully exposed, 5mg/kg BLM was punctured and perfused in the gap of the tracheal cricoid cartilage. The body position was rotated to make the drug evenly distributed in the lung tissues of the rat. The tissue was sutured layer by layer, and then the incision was disinfected. The rats in the Nor group were treated as the above way, and 0.9% normal saline solution was perfused via puncturing. The body weight, mental state, activity state, and death of the rats in each group were observed. In the Mox group, the rats were treated with Mox 2 days after modeling. The back-shu acupoints and the Xuxiao acupoints were marked according to *Experimental Acupuncture* and *Chinese Veterinary Acupuncture*. An appropriate amount of Vaseline was used to mark the points, and then alternate grain-sized moxibustion was performed. 5mg Mox was given to each acupoint 3 times once a day and 10 days were regarded as a course of treatment. An interval of 1 day was required between the two courses of treatment, and finally, a total of 3 courses of treatment were implemented. Rats in the BFQY group were given BFQY decoction through intragastric administration every day. Rats in the Mox+BFQY group were treated with Mox combined with BFQY decoction, and the treatment method was the same as mentioned above.

Pathological observation of lung tissues

The rats in each group were sacrificed by exsanguination from the femoral artery, and the alveolar lavage of the left lung was performed with normal saline after ligation of the main bronchus of the right lung. The lavage fluid was collected. The right lung tissue was fixed with

4% paraformaldehyde solution, and 2mm tissue was cut longitudinally at the hilum of the lung. After the tissue was washed, it was dehydrated with graded alcohol, hyalinized with xylene, and soaked in the melted paraffin liquid for 90 minutes. It was embedded and then became solidified, and the paraffin sections with a thickness of 4 μ m were made with a microtome.

Hematoxylin-eosin (HE) staining was performed. Tissue sections were deparaffinized with xylene and gradient alcohol solution and then were rinsed with running water and distilled water. They were stained with hematoxylin staining solution for 10 minutes and were treated with 1% hydrochloric acid alcohol solution for 10 minutes for tissue differentiation after rinse. 1% dilute ammonia solution was added to reverse blue after washing, and then 0.5% eosin staining solution was used for 2 minutes after rinsing again. Gradient alcohol solution was used for tissue dehydration, xylene solution was for tissue transparency, and neutral balsam solution was for sealing sheets.

Masson staining was described as follows. Routine dewaxing of the tissue was done, followed by treatment for 2 minutes with Ponceau red staining solution, 0.2% glacial acetic acid, 5% phosphomolybdic acid, and 0.2% glacial acetic acid. After that, methyl green staining was performed for 3 minutes and rinsed. After color separation with 95% ethanol solution, the tissue was dehydrated with gradient alcohol. The tissue was hyalinized in xylene, and the sheets were sealed with neutral balsam.

The degree of PF in lung tissue was assessed by the HE staining and Masson staining. The degree of alveolar inflammation was mainly defined as grade I-IV. The grade I indicated that the alveolar structure was normal. Grade II showed monocyte infiltration in the tissue, and about 20% of local alveolar septa were widened, but the overall structure was normal. Grade III suggested about 20%-50% of alveolar structural abnormalities, and the degree of abnormality in the alveoli closer to the pleura is severer. The grade IV meant there were more than 50% of alveolar structural abnormalities with a small number of inflammatory cells or hemorrhagic lesions in the alveolar space. The degree of PF was also classified into grade I-grade IV. Grade I indicated the normal lung tissue. Grade II showed fibrosis in about 20% of the lung tissue. Grade III was observed with fibrosis in about 20% to 50% of the lung tissue. Grade IV was shown that more than 50% of the tissue was fibrotic, and the structure of the alveoli was disorganized.

Determination of lung coefficient and the contents of hydroxyproline (HYP), glutathione (GSH), and malondialdehyde (MDA) in the tissue

After the rats were killed, the lung tissue was weighed. The lung coefficient was calculated according to the following equation: Lung coefficient = Wet lung weight/Body weight.

The contents of HYP, GSH, and MDA in rat lung tissue were detected by enzyme-linked immunosorbent assay (ELISA) in accordance with the instructions of the kit for detecting the contents in animal tissue.

Determination of messenger ribonucleic acid (mRNA) expression of NF- κ B p65, TGF- β 1, Smad2, and Smad7 in lung tissue

Total ribonucleic acid (RNA) was extracted from rat

Table 1. Quantitative primer information of target genes.

Target genes	Primer sequence (5'→3')	Product size (bp)
NF-κB p65	F: TGACCCCTGTCTCTCGCAT	400
	R: GGTCTCGTAGGTCCTTTTGGC	
TGF-β1	F: GAGAGCCCTGGATACCAACTACTG	173
	R: GTGTGTCCAGGCTCCAAATGTAG	
Smad2	F: AAGCCATCACCCTCAGAATTG	100
	R: CACTGATCTACCGTATTTGCTGT	
Smad7	F: GCATTCCTCGGAAGTCAAGAG	225
	R: CCAGGGGCCAGATAATTCGT	
β-actin	F: TCAGGTCATCACTATCGGCAAT	432
	R: AAAGAAAGGGTGTAAAACGCA	

lung tissue by the Trizol method. The purity, concentration, and integrity of the extracted RNA were detected by 1% agarose gel electrophoresis and Nanodrop spectrophotometer. The complementary deoxyribonucleic acid (cDNA) was synthesized according to the instructions of the SuperScript IV first-strand cDNA synthesis kit. The expression levels of NF-κB p65, TGF-β1, Smad2, Smad7, and β-actin gene were detected by real-time fluorescence quantitative polymerase chain reaction (PCR) in line with the instructions of the TaqMan gene expression detection kit. The primer information for quantitative detection of the target genes is shown in Table 1. As the β-actin was taken as the internal reference gene, the 2^{-ΔΔCt} method was used to calculate the relative expression levels of other target genes.

Determination of protein expression of NF-κB p65, TGF-β1, Smad2, and Smad7 in lung tissue

After the lung tissue was cut into small pieces, RIPA cell lysate buffer was added for tissue homogenization, and the total tissue protein was extracted on ice. The quantitative detection of protein concentration was performed with the bicinchoninic acid method, and the protein concentration was adjusted. Proteins were prepared and subjected to sodium dodecyl sulfate-polyacrylamide gel electrophoresis (SDS-PAGE), separated and transferred to polyvinylidene fluoride membranes. Mouse monoclonal antibody NF-κB p65 (1:1000), rabbit monoclonal antibody TGF-β1 (1:1000), rabbit monoclonal antibody Smad2 (1:1000), rabbit monoclonal antibody Smad7 (1:1000), and rabbit monoclonal antibody β-actin (1:5000) primary antibody was added as primary antibodies. They were incubated overnight in a 4°C refrigerator. Horseradish peroxidase-labeled rabbit-antibody rat immune globulin G (IgG) (1:5000) was then added as the secondary antibody and was incubated for 1h at room temperature. After being blocked with a blocking solution containing 5% nonfat milk powder, the color of the target protein bands was developed according to the ECL color development instructions. The protein bands were photographed in a gel imaging system, and the gray value was quantitatively detected using ImageJ software. β-actin was chosen as the internal reference gene, and the relative expression levels of other target gene proteins were detected by western blot.

Statistical processing

All experimental data were expressed as mean ± standard deviation (mean ± sd), and the significant difference

of each index among groups was detected through the one-way analysis of variance in SPSS19.0. $P < 0.05$ was considered to be statistically significant.

Results

General analysis of rats

90 male SD rats were chosen as the research objects, 10 of which were taken into the Nor group. The rest of the rats were prepared as PF models. The rats in the Nor group were very sensitive, with uniform breathing, good appetite, and great gloss of their hair. After being prepared as PF models, it can be observed that the breathing frequency of the rats was shortened, the thoracic cage floated significantly during breathing, and there was a frog croaking sound in the early stage. As time went on, the model rats became depressed, lost appetite, and had sparse and dull hair. The rats in different treatment groups suffered from a little bit of shortness of breath, but the mental, breathing, and appetite conditions were significantly improved compared with the rats in the PF model group.

The changes of rat body weight were analyzed at modeling, 3d, 7d, 14d, and 30d after treatment, and the results were shown in Figure 1. It was suggested that there was no significant difference in the body weight of the rats in each group 3 days after treatment ($P > 0.05$). With the increase of time, the body weight showed an increasing trend in each group. The body weight of the rats in the Nor group increased the fastest, followed by that in the Mox+BFQY group, while the PF group had the slowest weight gain.

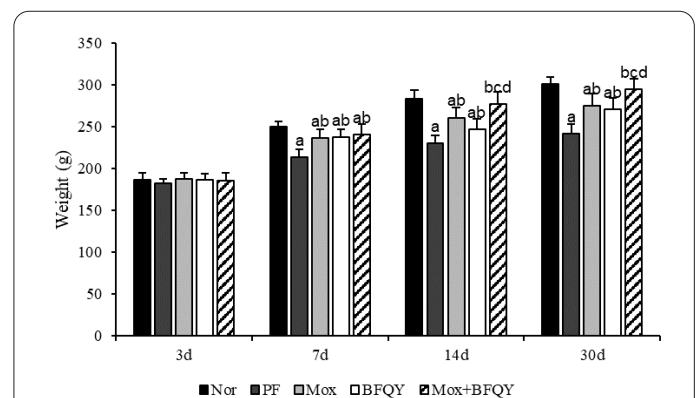


Figure 1. Body weight changes of rats in each group at different time points. (Compared with the data in Nor group, ^a $P < 0.05$; compared with those in PF group, ^b $P < 0.05$; and compared with those in Mox group and BFQY group, ^c $P < 0.05$ and ^d $P < 0.05$, respectively.)

Compared with those in the Nor group, the body weight of the rats in the PF group, Mox group, and BFQY group decreased significantly 7d, 14d, and 30d after treatment ($P<0.05$). The body weight of the rats in the Mox, BFQY and Mox+BFQY groups increased significantly 7d, 14d, and 30d after treatment ($P<0.05$) compared to those in the PF group. No significant difference was discovered in the body weight of rats in the Mox group and the BFQY group at each time point ($P>0.05$). Compared with the data in the Mox group and the BFQY group, the body weight in the Mox+BFQY group was significantly increased ($P<0.05$). It was shown with no significant difference in body weight between the Nor group and Mox+BFQY group 14d and 30d after treatment ($P>0.05$).

Changes in rat lung coefficient

The lung coefficient of the rats in each group was detected and compared, and the results are shown in Figure 2. Compared with that of the Nor group, the lung coefficient of the rats in the PF group, the Mox group, and the BFQY group were significantly increased ($P<0.05$); Compared with that of the PF group, it in the Mox, the BFQY, and the Mox+BFQY groups was significantly decreased ($P<0.05$). There was no significant difference in lung coefficient between the Mox group and the BFQY group ($P>0.05$). The lung coefficient of the Mox+BFQY group was greatly lowered ($P<0.05$) compared with those of the Mox group and BFQY group. There was also no significant difference in lung coefficient between the Nor group and the Mox+BFQY group ($P>0.05$).

HE staining observation of rat lung tissue under the optical microscope

HE staining was adopted to analyze the changes in the structure of the lung tissue of the rats in each group, and the alveolar inflammatory response was scored. The results are shown in Figure 3. A large number of inflammatory cells were exuded from the alveolar cavity of the lung tissue in the PF group, and collagen deposition appeared in the lung interstitium. The lung tissue structure of rats in all the Mox group, BFQY group, and Mox+BFQY group was presented with a significant improvement, and the improvement in the Mox+BFQY group was the most obvious. The alveolar inflammation scores in different groups were

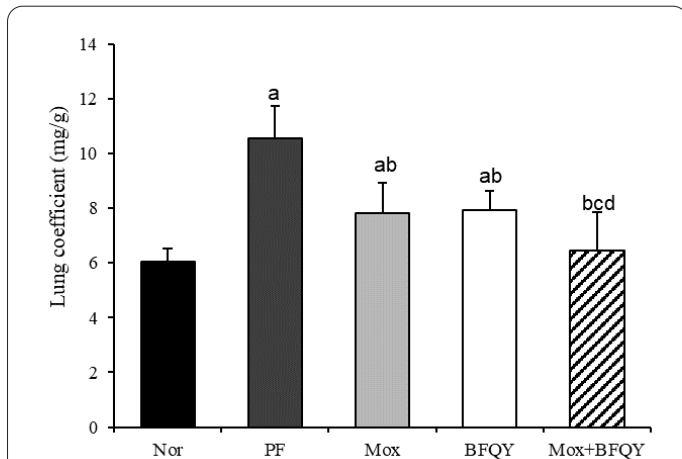


Figure 2. Changes in lung coefficient of rats in each group. (^a $P<0.05$, ^b $P<0.05$, ^c $P<0.05$, and ^d $P<0.05$ suggested a significant difference compared with those of the Nor group, PF group, Mox group, and BFQY group, respectively.)

compared. The scores of the rats in the PF group, the Mox group, and the BFQY group were significantly increased ($P<0.05$) compared with that in the Nor group. Compared with that of the PF group, that of the Mox, BFQY, and Mox+BFQY groups was significantly decreased ($P<0.05$). There was no significant difference in the scores between the Mox group and the BFQY group ($P>0.05$). The score was significantly lower in the Mox+BFQY group compared with that in the Mox group as well as the BFQY group ($P<0.05$). The difference in the score between the Nor group and the Mox+BFQY group was not significant ($P>0.05$).

Masson staining observation of rat lung tissue under the optical microscope

Masson staining was to observe the changes in the degree of PF in the lung tissue of rats and to score the degree of PF. It was shown in Figure 4 that collagen fibers in the pulmonary interstitium and bronchial tissues of the rats increased significantly in the PF group, and a large number of pulmonary interstitial collagen fibers were shown in a sheet-like distribution. In the Mox, BFQY, and Mox+BFQY groups, the degree of lung tissue PF was significantly improved; and that in the Mox+BFQY group had the most obvious improvement. In terms of the alveolar inflammation scores, the PF scores of the PF, the Mox, and the BFQY groups were significantly greater than

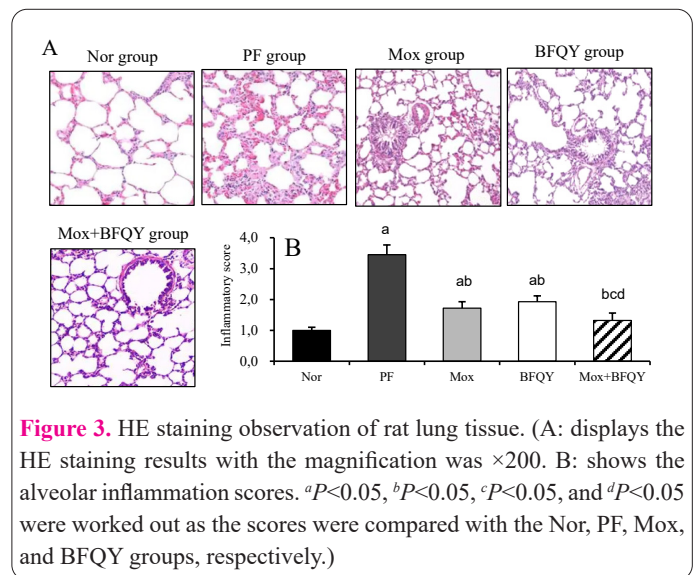


Figure 3. HE staining observation of rat lung tissue. (A: displays the HE staining results with the magnification was $\times 200$. B: shows the alveolar inflammation scores. ^a $P<0.05$, ^b $P<0.05$, ^c $P<0.05$, and ^d $P<0.05$ were worked out as the scores were compared with the Nor, PF, Mox, and BFQY groups, respectively.)

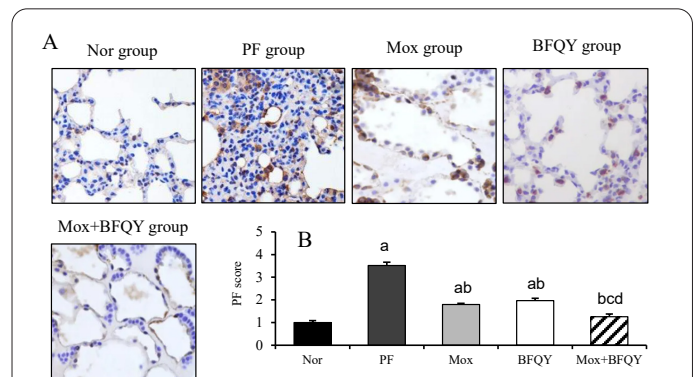


Figure 4. Masson staining observation of rat lung tissue. (A: presented the Masson staining observation, as the magnification was $\times 200$. B: displayed the score of the degree of PF. Compared with the score in Nor group, PF group, Mox group, and BFQY group, it could be obtained that ^a $P<0.05$, ^b $P<0.05$, ^c $P<0.05$, and ^d $P<0.05$, respectively.)

that of the Nor group ($P < 0.05$). While those of the Mox, the BFQY, and the Mox+BFQY groups were significantly lower than that of the PF group ($P < 0.05$). There was no significant difference in the PF scores between the Mox and BFQY groups ($P > 0.05$). The score of the Mox+BFQY group was also significantly lower than those of the Mox and BFQY groups ($P < 0.05$). No significant difference in the PF score between the Nor and the Mox+BFQY groups ($P > 0.05$).

Changes in HYP, GSH, and MDA contents in rat lung tissue

The contents of HYP, GSH, and MDA in rat lung tissue were detected, and the differences in them are shown in Figure 5. Compared with those in the Nor group, the contents of HYP, GSH, and MDA in the lungs of the rats in the PF group, Mox group and BFQY group were significantly higher ($P < 0.05$). The contents of HYP, GSH and MDA were significantly lower in the Mox, BFQY, and Mox+BFQY groups than those in the PF group ($P < 0.05$). However, there was no significant difference in the contents between the Mox group and the BFQY group ($P > 0.05$), as well as between the Nor group and the Mox+BFQY group ($P > 0.05$). The contents of HYP, GSH and MDA in the lungs of rats were significantly lower in the Mox+BFQY group than those of the Mox group and the BFQY group ($P < 0.05$).

mRNA expression levels of NF-κB p65, TGF-β1, Smad2, and Smad7 in rat lung tissue

The mRNA expression levels of NF-κB p65, TGF-β1, Smad2, and Smad7 in the lung tissue of the rats in each group were detected, as the results were shown in Figure 6. Compared with those in the Nor group, the mRNA expression levels of NF-κB p65, TGF-β1, and Smad2 in the lung tissue of the rats in the PF, Mox, and BFQY groups were significantly higher, and the expression of Smad7 was significantly lower ($P < 0.05$). The expression levels of NF-κB p65, TGF-β1, and Smad2 in the Mox group, BFQY group and Mox+BFQY group were significantly decreased, while the expression of Smad7 was significantly increased ($P < 0.05$), as those were compared to those in PF group. All the four mRNA expression levels in the Mox group were not significantly different from those in the BFQY group ($P > 0.05$). Compared with those in the Mox group and the BFQY group, the Mox+BFQY group showed significantly lower NF-κB p65, TGF-β1, and Smad2, but the significantly higher Smad7 in the lung tissue of the rats ($P < 0.05$). It was observed with no significant difference in the mRNA expression levels of all the NF-κB p65, TGF-β1, Smad2, and Smad7 between the Nor group and the Mox+BFQY group ($P > 0.05$).

Protein expression levels of NF-κB p65, TGF-β1, Smad2, and Smad7 in rat lung tissue

The protein expression levels of NF-κB p65, TGF-β1, Smad2, and Smad7 were detected in the lung tissue of the rats, and the results were shown in Figure 7. The expression levels of NF-κB p65, TGF-β1, and Smad2 proteins in the PF, Mox, and BFQY groups were significantly higher than those in the Nor group, while the expression of Smad7 was significantly lower ($P < 0.05$). The expression levels of NF-κB p65, TGF-β1, and Smad2 in the Mox, BFQY, and Mox+BFQY groups were significantly lower than those

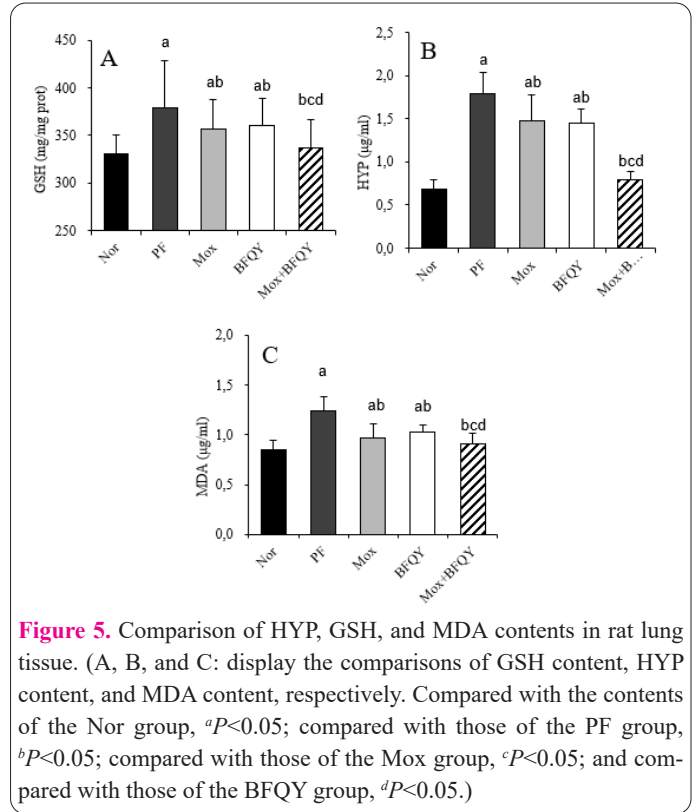


Figure 5. Comparison of HYP, GSH, and MDA contents in rat lung tissue. (A, B, and C: display the comparisons of GSH content, HYP content, and MDA content, respectively. Compared with the contents of the Nor group, ^a $P < 0.05$; compared with those of the PF group, ^b $P < 0.05$; compared with those of the Mox group, ^c $P < 0.05$; and compared with those of the BFQY group, ^d $P < 0.05$.)

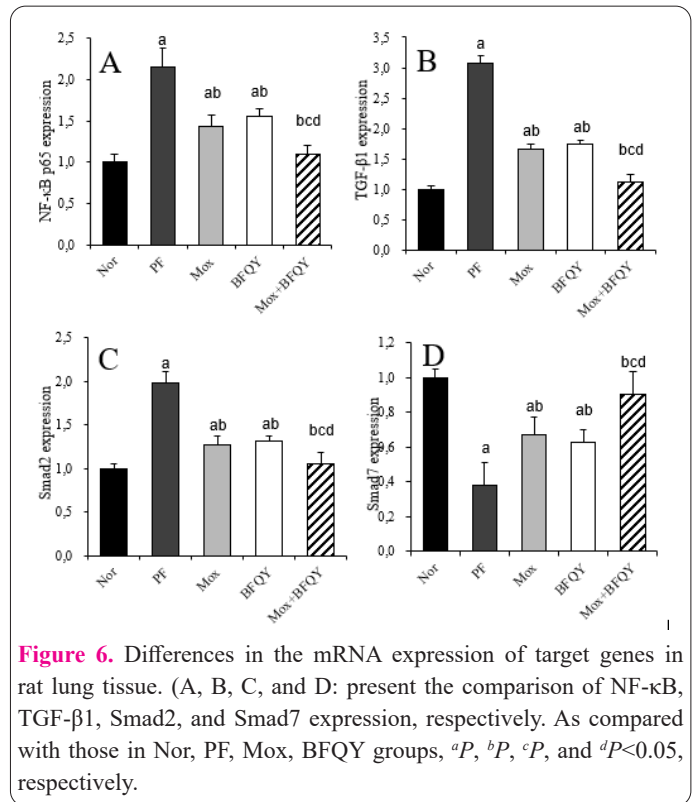


Figure 6. Differences in the mRNA expression of target genes in rat lung tissue. (A, B, C, and D: present the comparison of NF-κB, TGF-β1, Smad2, and Smad7 expression, respectively. As compared with those in Nor, PF, Mox, BFQY groups, ^a P , ^b P , ^c P , and ^d $P < 0.05$, respectively.

in the PF group while the expression of Smad7 was significantly increased ($P < 0.05$). The expression levels of the four proteins were not significantly different between the Mox and BFQY groups ($P > 0.05$). In the Mox+BFQY group, the level of NF-κB p65, TGF-β1, and Smad2 were significantly decreased, and the expression of Smad7 was significantly increased than those of the Mox group and the BFQY group ($P < 0.05$). No significant difference was found in the four protein expression levels between the Nor group and the Mox+BFQY group ($P > 0.05$).

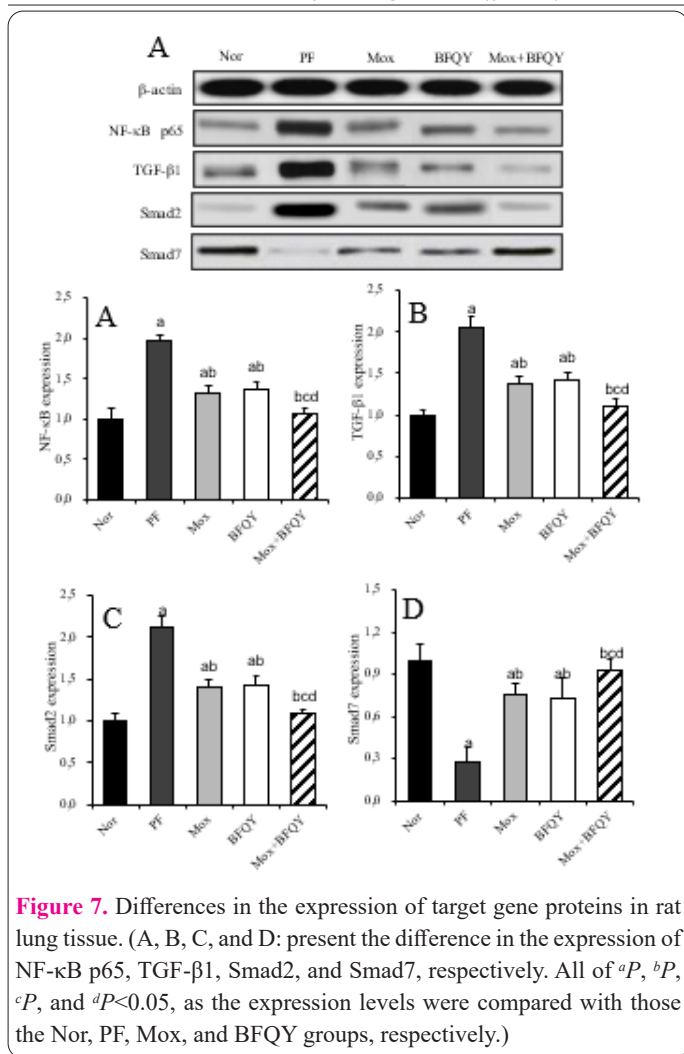


Figure 7. Differences in the expression of target gene proteins in rat lung tissue. (A, B, C, and D: present the difference in the expression of NF- κ B p65, TGF- β 1, Smad2, and Smad7, respectively. All of ^a*P*, ^b*P*, ^c*P*, and ^d*P*<0.05, as the expression levels were compared with those the Nor, PF, Mox, and BFQY groups, respectively.)

Discussion

The pathogenesis of PF is not clear now, and there are many methods for preparing PF models, among which the most common method is puncture perfusion with BLM (11). The pathological changes of the PF model prepared by BLM are very close to those of PF patients (12). Therefore, the rat PF models were prepared with BLM, and lung tissue sections were also prepared. With HE and Masson staining, it was found that a large number of inflammatory cells exuded from the alveoli of the model rats, and the degree of PF was deepened. Afterwards, the inflammatory response and the degree of PF in the rat lung tissue were scored, and those in the lung tissue of the PF rats were shown to be significantly increased. Thus, the PF model preparation was successful, which was consistent with the results reported by Walters and Kleeberger (2008) (13).

In traditional Chinese medicine, it is believed that PF has a nature of the deficiency, with symptoms such as asthma, phlegm, and blood stasis blocking collaterals (14). PF is caused by the coagulation of phlegm and blood stasis and obstruction of lung collaterals (15), and Mox has the effect of dispelling blood stasis and dissipating nodules (16). The BFQY decoction can invigorate the lung and qi, promote blood circulation, and remove blood stasis, etc. It can be used in the treatment of lung diseases with qi deficiency and blood stasis syndrome (17). Thereby, the grain-sized Mox at back-shu acupoints and Xuxiao acupoints were combined with BFQY decoction to treat PF rats. The changes of lung inflammatory response, the de-

gree of PF, and the contents in the tissue of HYP, GSH, and MDA were detected after treatment. The results suggested that Mox, BFQY decoction and the combination of Mox and the medicine could improve the lung inflammatory response and the degree of fibrosis in PF rats, and the combined therapy had the best therapeutic effect. Normal lung tissue owns a fully functional antioxidant system, including GSH and MDA. The above indicators can reflect the degree of internal oxidation in the body and reflect the degree of cell damage indirectly (18). HYP is a product formed by the hydroxylation of proline residues in the α -peptide chain, which can indirectly reflect the content of collagen (19). From the results, the contents of HYP, GSH, and MDA in the lung tissue of the rats were significantly reduced after Mox, BFQY decoction treatment, and the combined therapy of Mox and medicine, and each index of the rats after the combined therapy almost recovered to the normal levels.

NF- κ B is the most widely studied nuclear transcription factor, which is involved in the occurrence and development of various lung diseases (20). The TGF- β 1/Smads signaling pathway can participate in the process of PF by acting on lung fibroblasts, regulating inflammatory responses, and activating transcription factors (21). Researches have confirmed that blocking TGF- β 1 signaling can effectively prevent the occurrence of PF (22). The different treatment methods were examined on the NF- κ B/TGF- β 1/Smads pathway in PF rats. The mRNA and protein expression levels of NF- κ B p65, TGF- β 1, and Smad2 were significantly decreased, but the mRNA and protein expression levels of Smad7 were significantly increased. Overexpression of TGF- β 1 can cause collagen deposition, extracellular matrix protein aggregation, etc., which in turn leads to fibrosis of the lung interstitium or pleura (23). The TGF- β 1 binding receptor will cause phosphorylation of Smad2 protein, while Smad7 is an inhibitory regulatory protein during TGF- β 1 signaling (24,25). The above results proved that Mox, BFQY decoction and the combination of Mox and medicine could alleviate the fibrosis process of lung tissue by regulating the NF- κ B/TGF- β 1/Smads pathway in the treatment of PF.

For the treatment of BLM-induced PF in rats, grain-sized Mox combined with BFQY decoction can relieve the process of PF and improve alveolar inflammatory response by regulating the NF- κ B/TGF- β 1/Smads pathway. Ultimately, the prevention and treatment of PF would be achieved. The results provided new research ideas for exploring the treatment of PF by Mox and traditional Chinese medicine decoctions and also gave a new reference for the clinical treatment methods for PF.

Acknowledgements

The research is supported by: 1.Natural Science Foundation of Heilongjiang Province (No.: LH2020H100); 2.Special Research Fund for Harbin Science and Technology Innovators (No.: 2017RAQXJ189); 3.Heilongjiang Scientific Research Project of Traditional Chinese Medicine (No.: ZHY2020-136); 4.Scientific Research Project of The State Administration of Traditional Chinese Medicine (No.: 2021ZYLCYJ09-3).

References

1. Velagacherla V, Mehta CH, Nayak Y, Nayak UY. Molecular pa-

- thways and role of epigenetics in the idiopathic pulmonary fibrosis. *Life Sci.* 2022 Jan 5;120283. doi: 10.1016/j.lfs.2021.120283. Epub ahead of print. PMID: 34998839.
2. Kim HJ, Snyder LD, Neely ML, Hellkamp AS, Hotchkiss DL, Morrison LD, Bender S, Leonard TB, Culver DA; IPF-PRO™ Registry investigators. Clinical Outcomes of Patients with Combined Idiopathic Pulmonary Fibrosis and Emphysema in the IPF-PRO Registry. *Lung.* 2022 Jan 7. doi: 10.1007/s00408-021-00506-x. Epub ahead of print. PMID: 34997268.
 3. Hou J, Ma T, Cao H, Chen Y, Wang C, Chen X, Xiang Z, Han X. TNF- α -induced NF- κ B activation promotes myofibroblast differentiation of LR-MSCs and exacerbates bleomycin-induced pulmonary fibrosis. *J Cell Physiol.* 2018 Mar;233(3):2409-2419. doi: 10.1002/jcp.26112. Epub 2017 Aug 25. PMID: 28731277.
 4. Imakura T, Toyoda Y, Sato S, Koyama K, Nishimura H, Kagawa K, Takahashi N, Naito N, Murakami K, Kawano H, Azuma M, Shinohara T, Nishioka Y. Distinct improvement of pulmonary function, ground-glass opacity, hypoxia and physical findings in an idiopathic pulmonary fibrosis patient after pirfenidone treatment : a case report with a review of the literature. *J Med Invest.* 2020;67(3.4):358-361. doi: 10.2152/jmi.67.358. PMID: 33148916.
 5. Ruan H, Lv Z, Liu S, Zhang L, Huang K, Gao S, Gan W, Liu X, Zhang S, Helian K, Li X, Zhou H, Yang C. Anlotinib attenuated bleomycin-induced pulmonary fibrosis via the TGF- β 1 signalling pathway. *J Pharm Pharmacol.* 2020 Jan;72(1):44-55. doi: 10.1111/jphp.13183. Epub 2019 Oct 28. PMID: 31659758.
 6. Peng L, Wen L, Shi QF, Gao F, Huang B, Meng J, Hu CP, Wang CM. Scutellarin ameliorates pulmonary fibrosis through inhibiting NF- κ B/NLRP3-mediated epithelial-mesenchymal transition and inflammation. *Cell Death Dis.* 2020 Nov 13;11(11):978. doi: 10.1038/s41419-020-03178-2. PMID: 33188176; PMCID: PMC7666141.
 7. Rasmi RR, Sakthivel KM, Guruvayoorappan C. NF- κ B inhibitors in treatment and prevention of lung cancer. *Biomed Pharmacother.* 2020 Oct;130:110569. doi: 10.1016/j.biopha.2020.110569. Epub 2020 Aug 1. PMID: 32750649.
 8. P KM, Sivashanmugam K, Kandasamy M, Subbiah R, Ravikumar V. Repurposing of histone deacetylase inhibitors: A promising strategy to combat pulmonary fibrosis promoted by TGF- β signalling in COVID-19 survivors. *Life Sci.* 2021 Feb 1;266:118883. doi: 10.1016/j.lfs.2020.118883. Epub 2020 Dec 11. PMID: 33316266; PMCID: PMC7831549.
 9. Zhang Y, Lu P, Qin H, Zhang Y, Sun X, Song X, Liu J, Peng H, Liu Y, Nwafor EO, Li J, Liu Z. Traditional Chinese medicine combined with pulmonary drug delivery system and idiopathic pulmonary fibrosis: Rationale and therapeutic potential. *Biomed Pharmacother.* 2021 Jan;133:111072. doi: 10.1016/j.biopha.2020.111072. Epub 2020 Dec 8. PMID: 33378971; PMCID: PMC7836923.
 10. Li B, Zhang Y, Yang QM. [Umbilical moxibustion for patients with idiopathic pulmonary fibrosis complicated with gastroesophageal reflux of lung-spleen qi deficiency]. *Zhongguo Zhen Jiu.* 2019 Mar 12;39(3):241-5. Chinese. doi: 10.13703/j.0255-2930.2019.03.004. PMID: 30942008.
 11. Smith ML. Update on Pulmonary Fibrosis: Not All Fibrosis Is Created Equally. *Arch Pathol Lab Med.* 2016 Mar;140(3):221-9. doi: 10.5858/arpa.2015-0288-SA. PMID: 26927716.
 12. Kamio K, Azuma A, Matsuda K, Usuki J, Inomata M, Morinaga A, Kashiwada T, Nishijima N, Itakura S, Kokuho N, Atsumi K, Hayashi H, Yamaguchi T, Fujita K, Saito Y, Abe S, Kubota K, Gemma A. Resolution of bleomycin-induced murine pulmonary fibrosis via a splenic lymphocyte subpopulation. *Respir Res.* 2018 Apr 24;19(1):71. doi: 10.1186/s12931-018-0783-2. PMID: 29690905; PMCID: PMC5978999.
 13. Walters DM, Kleeberger SR. Mouse models of bleomycin-induced pulmonary fibrosis. *Curr Protoc Pharmacol.* 2008 Mar;Chapter 5:Unit 5.46. doi: 10.1002/0471141755.ph0546s40. PMID: 22294226.
 14. Yu XQ, Yang SG, Xie Y, Li JS. Traditional Chinese medicine in the treatment of idiopathic pulmonary fibrosis based on syndrome differentiation: Study protocol of an exploratory trial. *J Integr Med.* 2020 Mar;18(2):163-168. doi: 10.1016/j.joim.2019.12.005. Epub 2019 Dec 27. PMID: 31928920.
 15. Yao CF, Jiang SL. [Prevention and treatment of pulmonary-fibrosis by traditional Chinese medicine]. *Zhong Xi Yi Jie He Xue Bao.* 2003 Sep;1(3):234-8. Chinese. doi: 10.3736/jcim20030327. PMID: 15339572.
 16. Li R, Li WJ, Cai YN, Li ZG, Luo Q, Zhou MJ, Li CX, Li FH, Liu MF. [Effects of moxibustion at Feishu (BL 13) and Gaohuang (BL 43) on expression of TGF-beta1 in the bleomycin -induced pulmonary fibrosis]. *Zhongguo Zhen Jiu.* 2005 Nov;25(11):790-2. Chinese. PMID: 16335208.
 17. Chi X, Wang S, Baloch Z, Zhang H, Li X, Zhang Z, Zhang H, Dong Z, Lu Y, Yu H, Ma K. Research progress on classical traditional Chinese medicine formula Lily Bulb and Rehmannia Decoction in the treatment of depression. *Biomed Pharmacother.* 2019 Apr;112:108616. doi: 10.1016/j.biopha.2019.108616. Epub 2019 Feb 16. PMID: 30780102.
 18. Liu L, Qian H, Yin H, He J, Zhang P, Wang Z. [Unsaturated fatty acid of Actinidia chinensis Planch seed oil enhances the antioxidative stress ability of rats with pulmonary fibrosis through activating Keap 1/Nrf 2 signaling pathway]. *Xi Bao Yu Fen Zi Mian Yi Xue Za Zhi.* 2016 Apr;32(4):479-83. Chinese. PMID: 27053614.
 19. Yin JN, Li YN, Gao Y, Li SB, Li JD. Andrographolide plays an important role in bleomycin-induced pulmonary fibrosis treatment. *Int J Clin Exp Med.* 2015 Aug 15;8(8):12374-81. PMID: 26550147; PMCID: PMC4612832.
 20. Song C, He L, Zhang J, Ma H, Yuan X, Hu G, Tao L, Zhang J, Meng J. Fluorofenidone attenuates pulmonary inflammation and fibrosis via inhibiting the activation of NALP3 inflammasome and IL-1 β /IL-1R1/MyD88/NF- κ B pathway. *J Cell Mol Med.* 2016 Nov;20(11):2064-2077. doi: 10.1111/jcmm.12898. Epub 2016 Jun 16. PMID: 27306439; PMCID: PMC5082399.
 21. Luo L, Wang CC, Song XP, Wang HM, Zhou H, Sun Y, Wang XK, Hou S, Pei FY. Suppression of SMOC2 reduces bleomycin (BLM)-induced pulmonary fibrosis by inhibition of TGF- β 1/SMADs pathway. *Biomed Pharmacother.* 2018 Sep;105:841-847. doi: 10.1016/j.biopha.2018.03.058. Epub 2018 Jun 18. PMID: 30021376.
 22. Park SA, Kim MJ, Park SY, Kim JS, Lee SJ, Woo HA, Kim DK, Nam JS, Sheen YY. EW-7197 inhibits hepatic, renal, and pulmonary fibrosis by blocking TGF- β /Smad and ROS signaling. *Cell Mol Life Sci.* 2015 May;72(10):2023-39. doi: 10.1007/s00018-014-1798-6. Epub 2014 Dec 9. PMID: 25487606.
 23. Mackinnon AC, Gibbons MA, Farnworth SL, Leffler H, Nilsson UJ, Delaine T, Simpson AJ, Forbes SJ, Hirani N, Gaudie J, Sethi T. Regulation of transforming growth factor- β 1-driven lung fibrosis by galectin-3. *Am J Respir Crit Care Med.* 2012 Mar 1;185(5):537-46. doi: 10.1164/rccm.201106-0965OC. Epub 2011 Nov 17. PMID: 22095546; PMCID: PMC3410728.
 24. El-Seedy A, Pasquet MC, Shafiek H, Morsi T, Kitzis A, Ladevèze V. Cystic Fibrosis Transmembrane Conductance Regulator (CFTR) gene mutations in North Egyptian population: implications for the genetic diagnosis in Egypt. *Cell Mol Biol (Noisy-le-grand).* 2016 Nov 30;62(13):21-28. doi: 10.14715/cmb/2016.62.13.5. PMID: 28040058.
 25. Lee CM, He CH, Park JW, Lee JH, Kamle S, Ma B, Akosman

B, Cotez R, Chen E, Zhou Y, Herzog EL, Ryu C, Peng X, Rosas IO, Poli S, Bostwick CF, Choi AM, Elias JA, Lee CG. Chitinase 1 regulates pulmonary fibrosis by modulating TGF- β /SMAD7

pathway via TGFBRAP1 and FOXO3. *Life Sci Alliance*. 2019 May 13;2(3):e201900350. doi: 10.26508/lsa.201900350. PMID: 31085559; PMCID: PMC6516052.